To grow or not to grow: Thermomagnetic behavior of α_s

Alejandro Ayala

Instituto de Ciencias Nucleares, UNAM

In collaboration with C. A. Dominguez, L. Hernández, S. Hernández, M. Loewe, D. Manreza, R. Zamora

May 1st, 2018

Overview

Magnetic fields in peripheral HICs

1. Generated in the middle of the interaction region by currents produced by the (charged) colliding nuclei.

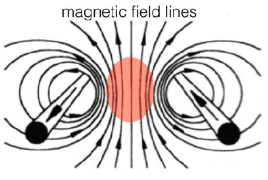

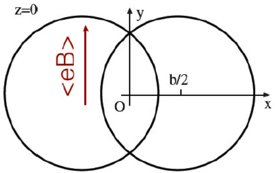

Time evolution of magnetic fields in HICs

The field intensity is a rapidly decreasing function of time

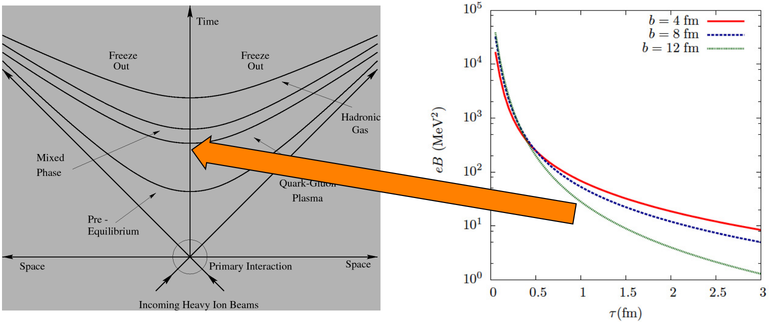

D. E. Kharzeev, L. D. McLerran, H. J. Warringa, Nucl. Phys. **A** 803, 227-253 (2008)

Inverse magnetic catalysis

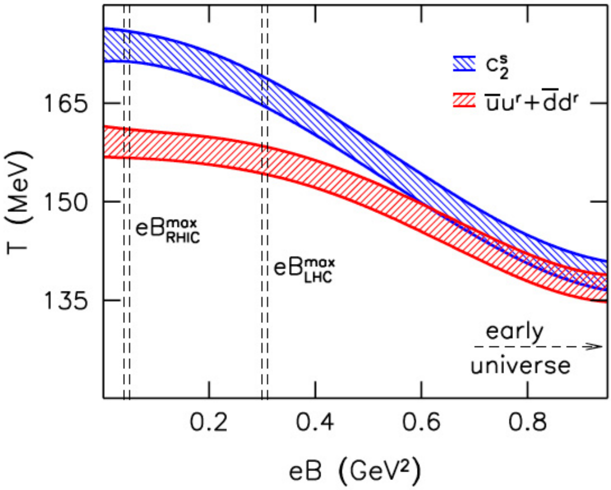

G. S. Bali *et al.*, JHEP **02** (2012) 044

Inverse magnetic catalysis

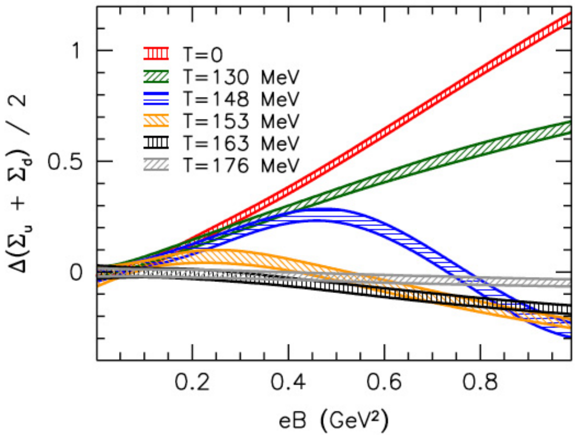

G. S. Bali *et al.*, Phys. Rev. D **86**, 071502 (2012)

Inverse magnetic catalysis

1. Competition between **valence** and **sea** quarks: G. Bali, F. Bruckmann, G. Endrodi, Z. Fodor, S. Katz, *et. al*, J. High Energy. Phys. 1202, 044 (2012)
2. Deconfinement transition for large N_c in the bag model: E. Fraga, J. Noronha, L. Palhares, Phys. Rev. D **87**, 114014 (2013)
3. Efective models **coupling constant decrement** with B: R. L. S. Farias, K. P. Gomes, G. Krein and M. B. Pinto, Phys. Rev. C **90**, 025203 (2014); M. Ferreira, P. Costa, O. Lourenço, T. Frederico, C. Providência, Phys. Rev. D **89**, 116011 (2014); A. A., M. Loewe, A. Mizher, R. Zamora, Phys. Rev. D **90**, 036001 (2014); A. A., M. Loewe, R. Zamora, Phys. Rev. D **91**, 016002
4. Paramagnetic phase (quarks and gluons) preferred over diamagnetic phase (pions): N. O. Agasian, S. M. Federov, Phys. Lett. B **663**, 445 (2008)

Running coupling constant

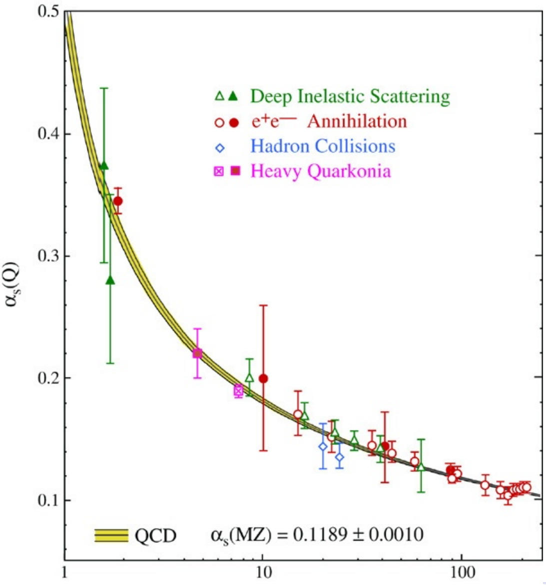

Photons from Gluon Fusion

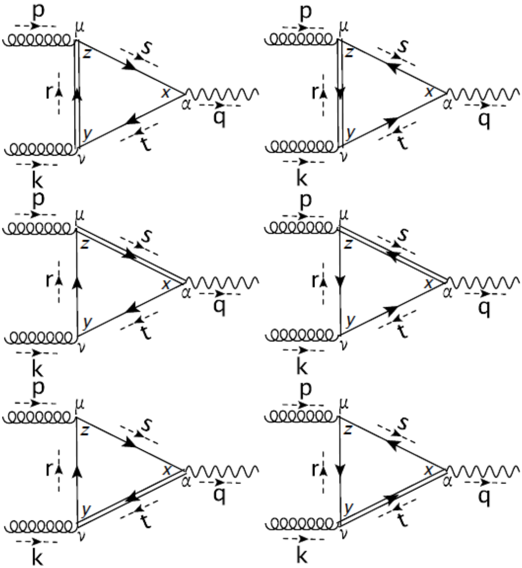

Photons from Gluon Fusion

A.A, M. J. D. Castaño Yepes, C. A. Dominguez, L. Hernández, S. Hernández, M. E. Tejeda-Yeomans, Phys. Rev. D **96**, 014023 (2017), Erratum: Phys.Rev. D **96**, 119901 (2017)

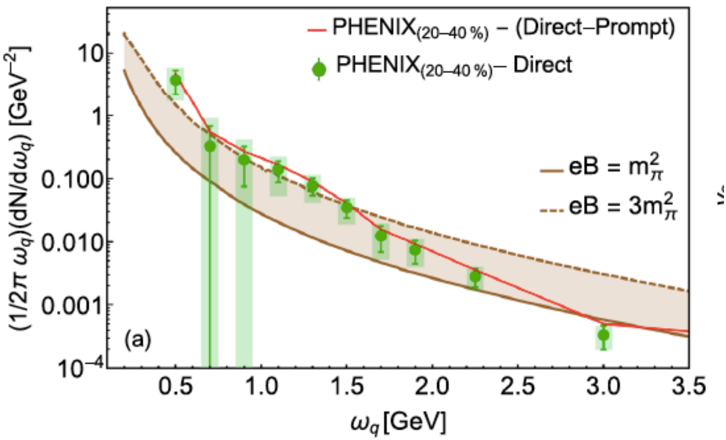

Photons from Gluon Fusion

A.A, M. J. D. Castaño Yepes, C. A. Dominguez, L. Hernández, S. Hernández, M. E. Tejeda-Yeomans, Phys. Rev. D **96**, 014023 (2017), Erratum: Phys.Rev. D **96**, 119901 (2017)

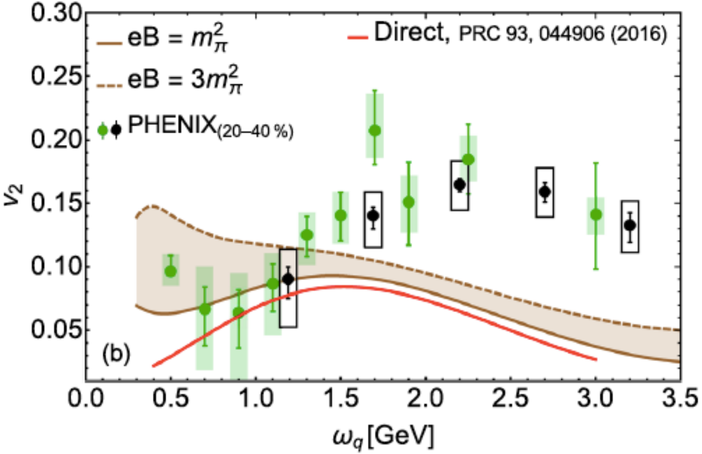

Magnetized phase diagram

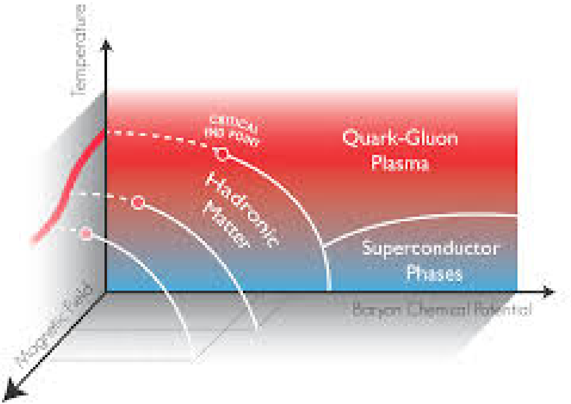

Chemical freeze-out curve closer to transition curve

P. Costa, M. Ferreira, D. P. Menezes, J. Moreira, C. Providência, Phys. Rev. D **92**, 036012 (2015)

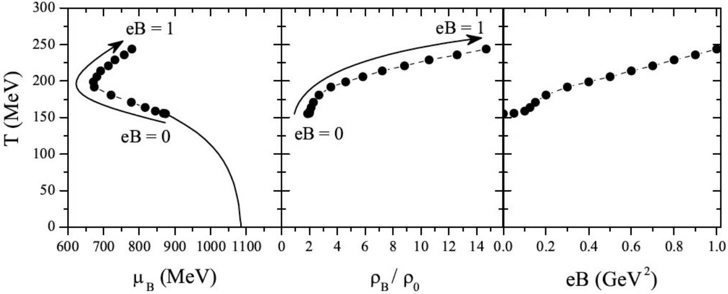

1. If the pseudo critical line for $B \neq 0$ **happens for higher temperatures and lower densities,** this can be closer to the chemical freeze-out curve.
2. Distance between CEP and freeze-out curve decreases.
3. **Signals of criticality can be revealed.**

Effective QCD model: Linear sigma model with quarks

- Effective QCD models (linear sigma model with quarks)

$$
\begin{aligned}
\mathcal{L} &= \frac{1}{2}(\partial_\mu \sigma)^2 + \frac{1}{2}(\partial_\mu \vec{\pi})^2 + \frac{a^2}{2}(\sigma^2 + \vec{\pi}^2) - \frac{\lambda}{4}(\sigma^2 + \vec{\pi}^2)^2 \\
&+ i\bar{\psi}\gamma^\mu \partial_\mu \psi - g\bar{\psi}(\sigma + i\gamma_5 \vec{\tau}\cdot\vec{\pi})\psi,
\end{aligned}
$$

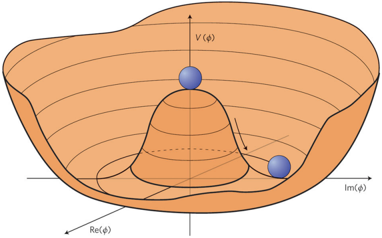

$$
\begin{aligned}
\sigma &\rightarrow \sigma + v, \\
m_\sigma^2 &= \frac{3}{4}\lambda v^2 - a^2, \\
m_\pi^2 &= \frac{1}{4}\lambda v^2 - a^2 \\
m_f &= gv \\
v_0 &= \sqrt{\frac{a^2}{\lambda}}
\end{aligned}
$$

Schwinger proper-time effective potential

$$
\begin{aligned}
V_b^{(1)} &= \frac{T}{2}\sum_n \int dm_b^2 \int \frac{d^3k}{(2\pi)^3} \int_0^\infty \frac{ds}{\cosh(q_b Bs)} \\
&\times \quad e^{-s\left(\omega_n^2 + k_3^2 + k_\perp^2 \frac{\tanh(q_b Bs)}{q_b Bs} + m_b^2\right)},
\end{aligned}
$$

$$
\begin{aligned}
V_f^{(1)} &= -\sum_{r=\pm 1} T \sum_n \int dm_f^2 \int \frac{d^3k}{(2\pi)^3} \int_0^\infty \frac{ds}{\cosh(q_f Bs)} \\
&\times \quad e^{-s\left(\tilde{\omega}_n^2 + k_3^2 + k_\perp^2 \frac{\tanh(q_f Bs)}{q_f Bs} + m_f^2 + r q_f B\right)},
\end{aligned}
$$

With couplings B-dependence, T_c decreases

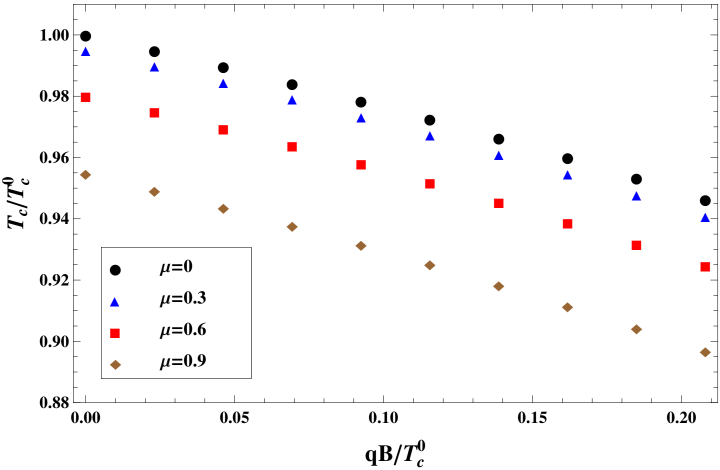

Without couplings B-dependence, T_c increases

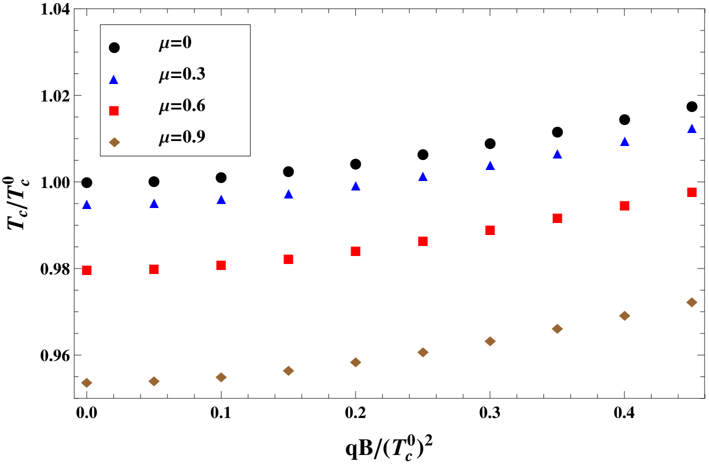

Magnetized effective phase diagram

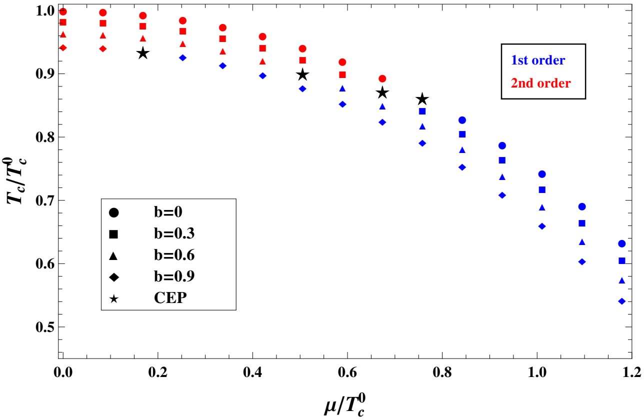

A. A., C. Dominguez, L. A. Hernández, M. Loewe, R. Zamora, Phys. Rev. D **92**, 096011 (2015)

QCD case: Quark-gluon vertex with a magnetic field

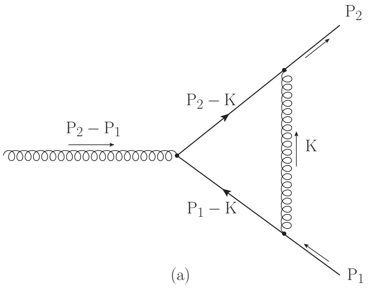

$$S(K) = \frac{m - \not{K}}{K^2 + m^2} - i\gamma_1\gamma_2 \frac{m - \not{K}_{\parallel}}{(K^2 + m^2)^2}(qB)$$

A. A., M. Loewe, J. Cobos-Martínez, M. E. Tejeda-Yeomans, R. Zamora, Phys. Rev. D **91**, 016007 (2015)

QCD case: **high temperature**

$$
\begin{aligned}
\delta\Gamma_\mu^{(a)} &= -ig^2(C_F - C_A/2)(qB)T\sum_n \int \frac{d^3k}{(2\pi)^3} \\
&\times \gamma_\nu \left[\gamma_1\gamma_2 \not{K}_\parallel \gamma_\mu \not{K} \widetilde{\Delta}(P_2 - K) \right.\\
&+ \left. \not{K}\gamma_\mu\gamma_1\gamma_2\not{K}_\parallel \widetilde{\Delta}(P_1 - K)\right]\gamma_\nu \\
&\times \Delta(K)\widetilde{\Delta}(P_2 - K)\widetilde{\Delta}(P_1 - K)
\end{aligned}
$$

$$
\begin{aligned}
\delta\Gamma_\mu^{(b)} &= -2ig^2\frac{C_A}{2}(qB)T\sum_n \int \frac{d^3k}{(2\pi)^3} \\
&\times \left[-\not{K}\gamma_1\gamma_2\not{K}_\parallel\gamma_\mu + 2\gamma_\nu\gamma_1\gamma_2\not{K}_\parallel\gamma_\nu K_\mu \right.\\
&- \left. \gamma_\mu\gamma_1\gamma_2\not{K}_\parallel\not{K}\right] \\
&\times \widetilde{\Delta}(K)^2\Delta(P_1 - K)\Delta(P_2 - K).
\end{aligned}
$$

QCD coupling as a function of B **high temperature**

$$\delta\vec{\Gamma}_{\parallel}(p_0) = \left(\frac{2}{3p_0^2}\right) 4g^2 C_F M^2(T, m, qB)\vec{\gamma}_{\parallel}\Sigma_3$$

$$M^2(T, m, qB) = \frac{qB}{16\pi^2}\left[\ln(2) - \frac{\pi}{2}\frac{T}{m}\right].$$

$$g_{\rm eff}^{\rm therm} = g\left[1 - \frac{m_f^2}{T^2} + \left(\frac{8}{3T^2}\right) g^2 C_F M^2(T, m_f, qB)\right],$$

QCD coupling as a function of B **zero temperature**

$$
\begin{aligned}
\delta\Gamma^{\mu}_{(a)} &= ig^3(qB)\left(C_F - \frac{C_A}{2}\right)\int \frac{d^4k}{(2\pi)^4}\frac{1}{k^2} \\
&\times \left\{\gamma^{\nu}\frac{(\not{p}_2 - \not{k})}{(p_2-k)^2}\gamma^{\mu}\frac{\gamma_1\gamma_2\left[\gamma\cdot(p_1-k)\right]_{\parallel}}{(p_1-k)^4}\gamma_{\nu}\right. \\
&+ \left.\gamma^{\nu}\frac{\gamma_1\gamma_2\left[\gamma\cdot(p_2-k)\right]_{\parallel}}{(p_2-k)^4}\gamma^{\mu}\frac{(\not{p}_1 - \not{k})}{(p_1-k)^2}\gamma_{\nu}\right\},
\end{aligned}
$$

$$
\begin{aligned}
\delta\Gamma^{\mu}_{(b)} &= -2ig^3(qB)\frac{C_A}{2}\int \frac{d^4k}{(2\pi)^4}\frac{1}{k^4}\left[g^{\mu\nu}(2p_2-p_1-k)^{\rho}\right. \\
&+ \left. g^{\nu\rho}(2k-p_2-p_1)^{\mu} + g^{\rho\mu}(2p_1-k-p_2)^{\nu}\right] \\
&\times \gamma_{\rho}\frac{\gamma_1\gamma_2(\gamma\cdot k)_{\parallel}}{(p_2-k)^2(p_1-k)^2}\gamma_{\nu},
\end{aligned}
$$

Quark-gluon vertex satisfies Ward-Takahashi identity with quark self-energy in the presence of weak B-fields

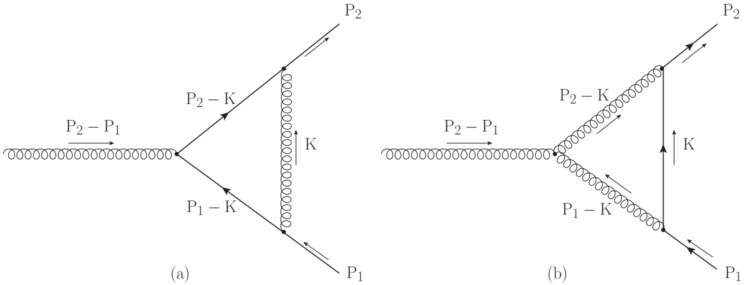

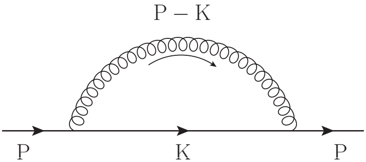

QCD coupling grows (decreases) at zero (high) T as a function of B

$$
\begin{aligned}
g_{\text{eff}}^{\text{vac}} &= g - \left[g^2 \frac{1}{3\pi^2} \frac{q\vec{\Sigma}\cdot\vec{B}}{Q^2} \right] \\
&\times \left\{ \left(C_F - \frac{C_A}{2} \right) [1 + \ln(4)] + \frac{C_A}{5} [-1 + \ln(4)] \right\} \\
&= g - \left[g^2 \frac{1}{3\pi^2} \frac{q\vec{\Sigma}\cdot\vec{B}}{Q^2} \right] \\
&\times \left\{ [1 + \ln(4)]\, C_F - \frac{[7 + 3\ln(4)]}{10} C_A \right\}. \\
C_F &= \frac{N^2 - 1}{2N} \qquad C_A = N
\end{aligned}
$$

For $N = 3$, $g_{\text{eff}}^{\text{vac}}$ **grows** whereas $g_{\text{eff}}^{\text{therm}}$ **decreases** with B.

RGE

- Let $\Pi(q^2; T, |eB|; \alpha_s)$ be the un-renormalized coefficient of a given tensor structure upon which the gluon polarization can be decomposed at finite temperature T and in the presence of a constant magnetic field $|eB|$.
- The statement that Π should be independent of this scale is provided by the RGE

$$\left(\mu\frac{\partial}{\partial\mu} + \alpha_s\beta(\alpha_s)\frac{\partial}{\partial\alpha_s} - \gamma\right)\Pi(q^2; T, eB; \alpha_s) = 0$$

- where $\beta(\alpha_s)$ is the QCD beta function defined by

$$\alpha_s\beta(\alpha_s) = \mu\frac{\partial\alpha_s}{\partial\mu}$$

- and $\gamma = \mu\frac{\partial}{\partial\mu}\ln Z^{-1}$ is the anomalous dimension

Beta function

- It is well known that the QCD beta function is negative and that to one-loop level it is given by

$$\beta(\alpha_s) \;=\; -b_1\alpha_s, \quad b_1 = \frac{1}{12\pi}\left(11N_c - 2N_f\right),$$

- with N_c the number of colors and N_f the number of active flavors.

Running of α_s with Q^2

- To set up the stage, first recall how the usual evolution of the strong coupling with the momentum scale is established. Consider that the only energy scale in the function Π is q^2

$$\left(\mu\frac{\partial}{\partial\mu}+\alpha_s\beta(\alpha_s)\frac{\partial}{\partial\alpha_s}-\gamma\right)\Pi(q^2;\alpha_s)=0.$$

- introduce the variable

$$t=\ln(Q^2/\mu^2),$$

- where Q^2 is the momentum transfered in a given process. Notice that the reference scale μ^2 is usually large enough, so as to make sure that the calculation is well within the perturbative domain, therefore $Q^2<\mu^2$.

Running of α_s with Q^2

- The RGE becomes

$$\left(-\frac{\partial}{\partial t} + \alpha_s \beta(\alpha_s)\frac{\partial}{\partial \alpha_s} - \gamma\right)\Pi(q^2;\alpha_s) = 0.$$

- The relation between the coupling values evaluated at Q^2 and the reference scale μ^2 as

$$\int_{t(Q^2=\mu^2)}^{t(Q^2)} dt = -\frac{1}{b_1}\int_{\alpha_s(Q^2=\mu^2)}^{\alpha_s(Q^2)} \frac{d\alpha_s}{\alpha_s^2}.$$

- Solving for $\alpha_s(Q^2)$, we obtain

$$\alpha_s(Q^2) = \frac{\alpha_s(\mu^2)}{1 + b_1 \alpha_s(\mu^2)\ln(Q^2/\mu^2)},$$

- From where it is seen that as Q^2 increases, the coupling decreases.

Running coupling constant

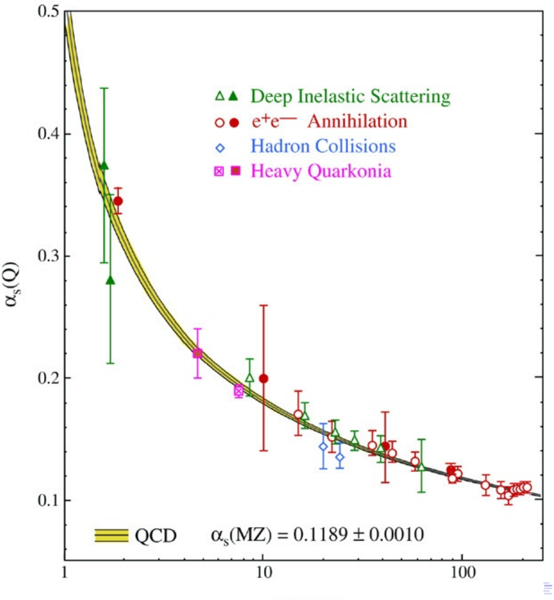

Gluon vacuum polarization weak field limit and $T = 0$

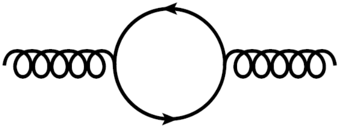

$$\Pi^{\mu\nu} = \Pi_{\parallel}\left(g_{\parallel}^{\mu\nu} - \frac{q_{\parallel}^{\mu} q_{\parallel}^{\nu}}{q_{\parallel}^2}\right) + \Pi_{\perp}\left(g_{\perp}^{\mu\nu} + \frac{q_{\perp}^{\mu} q_{\perp}^{\nu}}{q_{\perp}^2}\right)$$
$$+ \Pi_0\left[\left(g^{\mu\nu} - \frac{q^{\mu} q^{\nu}}{q^2}\right) - \left(g_{\parallel}^{\mu\nu} - \frac{q_{\parallel}^{\mu} q_{\parallel}^{\nu}}{q_{\parallel}^2}\right) - \left(g_{\perp}^{\mu\nu} + \frac{q_{\perp}^{\mu} q_{\perp}^{\nu}}{q_{\perp}^2}\right)\right],$$

$$\Pi_{\parallel} = -\alpha_s \frac{(eB)^2}{3\pi}\left(\frac{2q_{\parallel}^4}{q^6}\right)\sum_f q_f^2, \qquad \Pi_{\perp} = -\alpha_s \frac{(eB)^2}{3\pi}\left(\frac{2q_{\perp}^4}{q^6}\right)\sum_f q_f^2,$$

$$\Pi_0 = \alpha_s \frac{(eB)^2}{3\pi}\frac{(q_{\parallel}^2 q_{\perp}^2)}{q^6}\sum_f q_f^2.$$

Evolution equations

Consider $\Pi_{\parallel}$. Scale all energy factors by μ (the renormalization scale)

$$\Pi^{\parallel}_{\text{weak}} = \frac{2}{3}\frac{\alpha_s}{\pi}|eB|^2\left[\frac{(q_{\parallel}^2)^2}{(q^2)^3}\right], \\ = \mu^2\frac{\lambda_B^4}{\lambda_q^2}\frac{2}{3}\frac{\alpha_s}{\pi}(|eB|^2/\mu^4)\left[\frac{(q_{\parallel}^2/\mu^2)^2}{(q^2/\mu^2)^3}\right].$$

- Using the RGE, we get

$$\left(-\lambda_q\frac{\partial}{\partial\lambda_q}-\lambda_B\frac{\partial}{\partial\lambda_B}+\alpha_s\beta(\alpha_s)\frac{\partial}{\partial\alpha_s}-\tilde{\gamma}\right)\Pi^{\parallel}_{\text{weak}}=0,$$

- where $\tilde{\gamma}=\gamma-D$

Evolution equations

- Using the method of the characteristics, we can write

$$dt = -\frac{d\lambda_q}{\lambda_q}, \quad dt = -\frac{d\lambda_B}{\lambda_B},$$

- whose solutions are

$$\lambda_q = C_q e^{-t}, \quad \lambda_B = C_B e^{-t},$$

- where C_q and C_B are integration constants to be determined from the initial condition for the evolution. Upon combining, we can write

$$\lambda_q + \lambda_B \;=\; (C_q + C_B)e^{-t} = e^{-t},$$

Evolution equations

- For the subsequent evolution we take Q^2 fixed and thus we refer the evolution of $|eB|$ to the reference scale Q^2, namely, we take $\lambda_B = |eB|/Q^2$. Therefore, we can write

$$t = \ln\left(\frac{Q^2}{Q^2 + |eB|}\right).$$

- Notice that in this case the evolution energy scale appears in the denominator of the logarithmic function. Therefore the RGE becomes

$$\left(\frac{\partial}{\partial t} + \alpha_s \beta(\alpha_s)\frac{\partial}{\partial \alpha_s} - \tilde{\gamma}\right)\Pi^{\parallel}_{\text{weak}} = 0,$$

Evolution equations

- The relation between the coupling values evaluated at $|eB|$ and the reference scale Q^2 can be expressed as

$$\int_{t(\lambda_B=0)}^{t(\lambda_B=|eB|/Q^2)} dt = -\frac{1}{b_1}\int_{\alpha_s(Q^2)}^{\alpha_s(Q^2+|eB|)} \frac{d\alpha_s}{\alpha_s^2}.$$

- Solving for $\alpha_s(Q^2+|eB|)$, we obtain

$$\alpha_s(Q^2+|eB|) = \frac{\alpha_s(Q^2)}{1+b_1\alpha_s(Q^2)\ln\left(\frac{Q^2}{Q^2+|eB|}\right)}.$$

- We see that as the magnetic field intensity increases, the coupling increases with respect to its corresponding value at the reference scale Q^2.

Strong field limit

- For $|eB| > Q^2$ still for $T = 0$, in the Lowest Landau Level approximation

$$\begin{aligned}\Pi^{\|}_{\text{strong}} &= \frac{2}{3}\frac{\alpha_s}{\pi}|eB|e^{-q_\perp^2/2|eB|} \\ &= \mu^2\lambda_B^2\frac{2}{3}\frac{\alpha_s}{\pi}\left(\frac{|eB|}{\mu^2}\right)e^{-\left(\frac{\lambda_q^2}{\lambda_B^2}\right)(q_\perp^2/2|eB|)},\end{aligned}$$

- Upon using the RGE

$$\Big(-\lambda_q\frac{\partial}{\partial\lambda_q} - \lambda_B\frac{\partial}{\partial\lambda_B} + \alpha_s\beta(\alpha_s)\frac{\partial}{\partial\alpha_s} - \tilde{\gamma}\Big)\Pi^{\|}_{\text{strong}} = 0.$$

Evolution equations

- Using the same arguments as for the weak field case, which implies starting the evolution from the fixed scale $Q^2 < |eB|$, we once again obtain for the relation between the coupling evaluated at $|eB|$ and the reference scale Q^2

$$\alpha_s(|eB|) = \frac{\alpha_s(Q^2)}{1 + b_1 \alpha_s(Q^2) \ln\left(\frac{Q^2}{Q^2+|eB|}\right)}.$$

- These results show that for $T = 0$, α_s is an increasing function of $|eB|$, when referred to the scale Q^2.

Thermo-magnetic case

- We now turn to study the finite temperature case. Given that there is no need to assume a given hierarchy between T^2 and $|eB|$, the calculation is more straightforwardly performed when working in the LLL approximation.

$$
\begin{aligned}
\Pi_T^{\parallel} &= \frac{2}{3}\frac{\alpha_s}{\pi}|eB|e^{-q_\perp^2/2|eB|}\ln\left(\frac{m^2}{\pi^2 T^2}\right) \\
&= \mu^2\lambda_B^2\frac{2}{3}\frac{\alpha_s}{\pi}\left(\frac{|eB|}{\mu^2}\right)e^{-\left(\frac{\lambda_q^2}{\lambda_B^2}\right)(q_\perp^2/2|eB|)} \\
&\times \ln\left(\frac{\lambda_m^2 m^2/\mu^2}{\pi^2\lambda_T^2 T^2/\mu^2}\right),
\end{aligned}
$$

Thermo-magnetic case

- It is easy to check that this coefficient satisfies

$$\left(\mu\frac{\partial}{\partial\mu} + \sum_{i=q,B,m,T}\lambda_i\frac{\partial}{\partial\lambda_i} - D\right)\Pi_T^{\parallel} = 0$$

- and that upon using the RGE one obtains

$$\left(-\sum_{i=q,B,m,T}\lambda_i\frac{\partial}{\partial\lambda_i} + \alpha_s\beta(\alpha_s)\frac{\partial}{\partial\alpha_s} - \tilde{\gamma}\right)\Pi_T^{\parallel} = 0.$$

Thermo-magnetic case

- When $|eB|$ is the largest of the scales

$$\alpha_s(|eB|) = \frac{\alpha_s(Q^2 + \widetilde{T}^2)}{1 + b_1\alpha_s(Q^2 + \widetilde{T}^2)\ln\left(\frac{Q^2+T^2}{Q^2+T^2+|eB|}\right)},$$

- When T is the largest of the scales

$$\alpha_s(|eB|) = \frac{\alpha_s(Q^2 + \widetilde{|eB|})}{1 + b_1\alpha_s(Q^2 + \widetilde{|eB|})\ln\left(\frac{Q^2+|eB|}{Q^2+|eB|+T^2}\right)},$$

Thermo-magnetic evolution

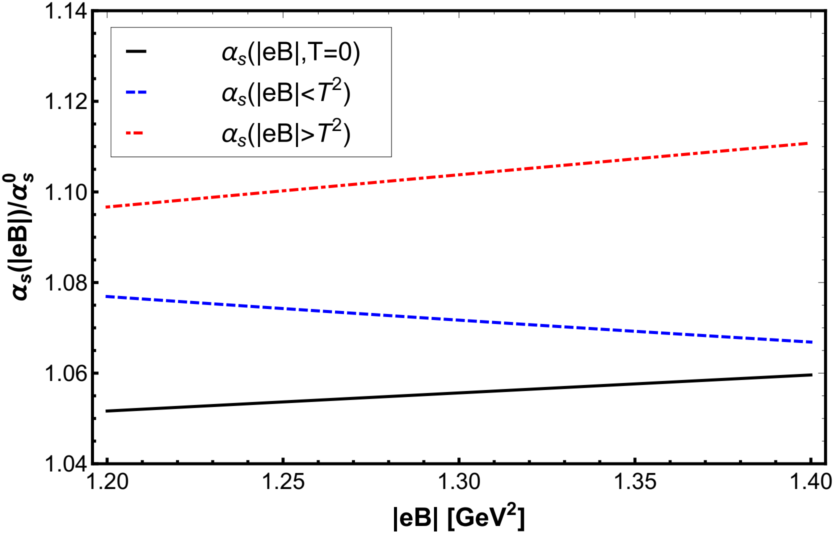

Conclusions

1. Magnetic fields provide extra handle to probe QCD properties under extreme conditions.
2. Effective model calculations show that magnetic field-induced changes in couplings describe **inverse magnetic catalysis.**
3. QCD quark-gluon vertex-B field dependent: Coupling decreases at high T and increases at zero T.
4. Effect due to subtle competition between the charges associated to quarks and gluons.
5. α_s shows a non-trivial evolution: Whereas at $T = 0$ it definitely increases with $|eB|$, at high T there is a turn over behavior and it decreases as eB increases.
6. The found evolution of α_s with T and $|eB|$ could help explain the inverse magnetic catalysis phenomenon.

THANKS!